Proceedings of GT2007
ASME Turbo Expo 2007: Power for Land, Sea and Air
May 14-17, 2007, Montreal, Canada

GT2007-28009

TOLERANCED DESIGNS OF COOLED TURBINE BLADES THROUGH PROBABILISTIC THERMAL ANALYSIS OF MANUFACTURING VARIABILITY

Curtis W. Moeckel*
Master's Student
Department of Aeronautics and Astronautics
Massachusetts Institute of Technology
Cambridge, Massachusetts 02139
Email: moeckel@alum.mit.edu

David L. Darmofal
Associate Professor
Department of Aeronautics and Astronautics
Massachusetts Institute of Technology
Cambridge, Massachusetts 02139
Email: darmofal@mit.edu

T. Robert Kingston
Technical Lead for Turbine Cooling
Rolls-Royce plc
PO Box 3 Filton, Bristol
BS34 7QE, United Kingdom
Email: robert.kingston@rolls-royce.com

Robert J. G. Norton
Chief Engineer, Turbines
Rolls-Royce Corporation
PO Box 420
Indianapolis, Indiana 46206-0420

ABSTRACT

Manufacturing variability is likely the primary cause of a large scatter in the life of gas turbine hot section components. This paper investigates manufacturing variability and its effect on first-stage turbine blades through the use of a parametric CAD model, automated CAD regeneration software, and a parametric finite element thermal model. The probabilistic approach used is substantiated due to differences that arise when input parameters vary at different levels, for example the engine-to-engine and blade-to-blade level. Schemes are proposed to improve robustness through tolerancing out input parameters in ranges of the distributions that make nonconformances more likely. A framework is presented for calculating the potential number of prevented non-conformances and the corresponding cost savings associated with various tolerancing schemes. Blade-to-blade cooling flow variability, especially as a result of film-hole diameter variability in critical locations, is identified as the most likely candidate for parameter tolerancing. More effective is a combined two-factor tolerancing scheme which additionally tolerances gas path temperature.

NOMENCLATURE

μ, σ Mean, standard deviation of parameter
T_3 Compressor discharge total temperature
T_{41} Turbine inlet total temperature
$RTDF$ Radial temperature distribution function
W_{41} Turbine mass flow rate
$m_{cool,blade}$ Blade cooling mass flow rate
D Diameter of film-cooling hole
t_{tbc} Thickness of thermal barrier coating
$coreshift$ Shift of core from nominal position
k Thermal conductivity, quasi-compressible loss coefficient
h Heat transfer coefficient
Bi Biot number
Re Reynolds number
$T_{average,section}$ Average metal temperature at a section
π Normalized profitability

*Currently: Engineer/Technologist, GE Aviation, Fan and Compressor Aerodynamics, curtis.moeckel@ge.com.

INTRODUCTION

Despite substantial progress in materials and cooling technology, turbine rotor inlet temperature has concurrently been increased to realize cycle performance improvements. As a result, first-stage turbine blades have traditionally been designed to operate with little margin relative to numerous criteria which may cause a non-conforming blade. The need for first-stage turbine blades to perform robustly is more important now than ever. With the introduction of "power by the hour" contracts, the manufacturer has assumed more responsibility for providing reliable power. In order to provide reliable power, turbine blade life must exhibit minimal scatter from part-to-part and the life-limiting blade must have a predictable and acceptable life, such that maintenance can be anticipated.

A first-stage turbine blade may non-conform in the field for a variety of reasons, including thermo-mechanical/low cycle fatigue, high cycle fatigue, creep, and environmental fatigue mechanisms including oxidation and corrosion. In addition to having to consider multiple possible mechanisms leading to non-conformances, it should be noted that life can be highly non-linear with respect to assumed loads. Also, the problem is even more complex since various failure mechanisms tend to interact with each other [1]. For example, a blade which is undergoing creep deformation in the field will not have the same low cycle fatigue life as a blade which is not susceptible to creep. Analyzing turbine hot section components in a probabilistic framework has been the topic of much previous research [1–7]. The capability to probabilistically predict the life of every turbine blade in an engine considering each possible failure regime simultaneously would be ideal. To the knowledge of the authors, a feasible multidisciplinary infrastructure to address this problem probabilistically has not yet been demonstrated. However, the computational expense of probabilistically predicting the temperature distribution of each blade within a fleet of engines is feasible even with modest computing resources. By assuming that certain non-conformance mechanisms can be traced back to temperature-related phenomenon within a blade, the problem is pared down to a level where investigations related to design robustness can be pursued. Specifically, this paper will investigate creep non-conformances since creep life is related to average section temperature.

This paper will present an investigation into the probabilistic behavior of cooled first-stage turbine blades of a hypothetical fleet of engines (500 engines consisting of 70 first-stage turbine blades each). This investigation is based upon a probabilistic finite element thermal analysis of a turbine blade including a parametric CAD master model allowing for core shift while also considering input parameters at both the blade-to-blade and the engine-to-engine level. Methods will be presented for the identification and ranking of key input parameters which affect the robustness of a first-stage turbine blade, despite the fact that these input parameters enter the problem at different levels, e.g. blade-to-blade and engine-to-engine levels. Then, a novel method of controlling the tails of select input distributions with the effect of improving the robustness of first-stage turbine blades will be presented. Finally, a cost model which substantiates the potential for cost savings by pursuing robust first-stage turbine blades will be presented.

MODEL OVERVIEW

A parameterized thermal model of a cooled first-stage turbine blade was developed to research the probabilistic behavior of a hypothetical fleet of engines. A representative (though hypothetical) convection and film-cooled first-stage turbine blade was provided by a turbine engine OEM (Rolls-Royce) as the baseline design for the project. For physical geometric changes in the blade, a parameterized UniGraphics NX3 model as shown in Figure 1 was created such that parameters like the core placement could be changed. The core placement and sectioning of each blade was handled in an automated fashion using CAPRI [8]. The ANSYS finite element package was used to develop both a multi-pass flow network model as shown in Figure 2 and a finite element thermal model of the blade consisting of five planar sections connected with a flow network which could transfer heat with the blade metal as shown in Figure 3. These parameterized models were set up in such a way that the input variables could be assigned values at random from statistical distributions describing the variability in the input parameters.

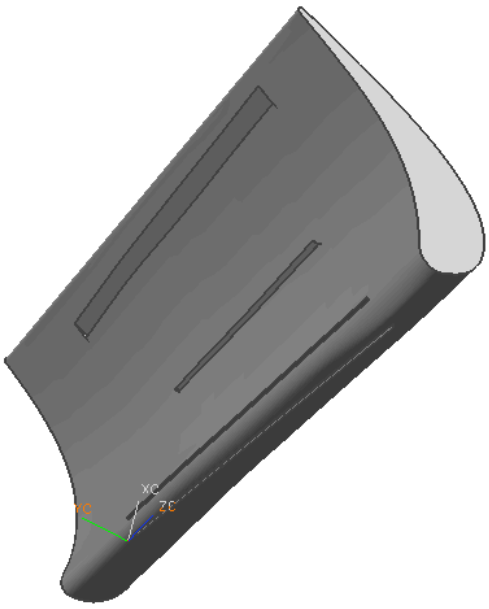

Figure 1: UniGraphics NX3 parameterized cooled turbine blade.

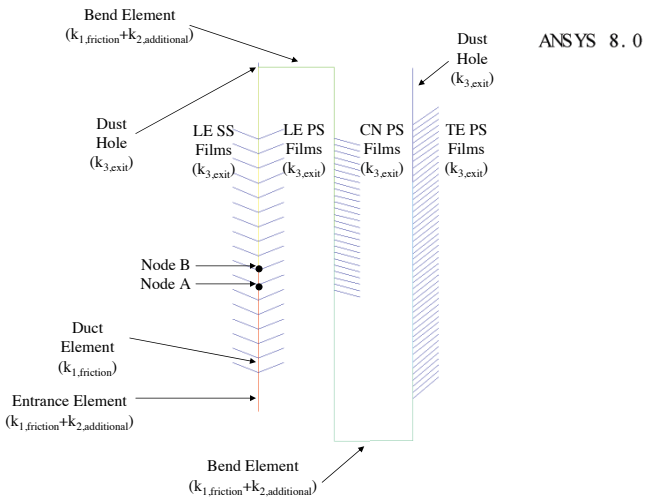

Figure 2: Multi-pass flow network model.

Figure 3: Two-dimensional model of cooled turbine blade.

PROBABILISTIC INPUT CONSIDERATIONS

The first step of both deterministic and probabilistic analyses of the temperature distribution of a cooled gas turbine blade is to determine the key input parameters which might affect the temperature distribution in the part. In a deterministic analysis, an engineer will often chose one value for each of the input parameters which the model requires. If a risk is inherent, sensitivity analyses might also be performed to consider the range of input parameters considered to be critical. However, in a probabilistic framework, a differentiation between uncertainty and variability as well as the type of distribution and level at which the deviation occurs must be determined.

There are two ways in which input parameters can differ from their single value representations used in practice (e.g. mean, most likely, assumed value). First, the uncertainty of a parameter can be characterized as the lack of knowledge relative to the true discrete value of each instance of the parameter. In contrast, the variability of a parameter is a measure of the range which the true discrete values of the parameter span for the population of interest.

In practice, some input parameters are inherently dominated by uncertainties while others are dominated by variabilities. For example, heat transfer coefficients are often dominated by uncertainty. Classical correlations, such as the Dittus-Boelter relation, may exhibit errors as large as 25%, while the complexity of more recent correlations can reduce the uncertainty to less than 10% [9]. In contrast, geometric features of a part are examples of parameters dominated by variability as a result of the manufacturing process. Using high precision measurement techniques (e.g. coordinate measuring machines) the variability of a feature from part-to-part is much greater than the uncertainty associated with the measurement.

Uncertainty tends to characterize the developmental phase of an engine program. When a developmental design is accepted as satisfactory and transitions into production, variabilities become of primary importance. If the production design is deemed unsatisfactory as a result of variability, the costs associated can include warranty claims, contractual costs, scrap, rework, redesign, and dissatisfied customers. Combining uncertainty and variability into the same analysis could lead to ambiguous conclusions, so the effects of each should be analyzed separately. The focus of this research will be on variability.

The levels at which parameters vary depends on how various units are grouped. For example, since each cooled turbine blade has a separate core around which the blade is formed, the deviation of the position of the core, *core shift*, is said to vary at the blade-to-blade level. That said, the tooling used to create the cores themselves may experience wear and have to be replaced or reworked after a certain number of batches. Thus wall thicknesses may have some variation at the blade batch-to-batch level. The recent research of Sidwell and Darmofal [6,10], which demonstrated that blade-to-blade variability in cooling flow was a main driver of oxidation damage, highlights the importance of considering variability at the blade-to-blade level. Possible levels of variability can include the blade-to-blade, engine-to-engine, blade batch-to-batch, engine batch-to-batch, and airline-to-airline levels. This paper will deal with simultaneously considering blade-to-blade and engine-to-engine variability.

INPUT PARAMETERS

The input parameters are presented in Table 1. The parameters are grouped into one of three categories: engine-to-engine cycle parameters, blade-to-blade flow network parameters, and blade-to-blade conduction parameters. Since this part is loosely based on industry experience, normalized values are presented.

Table 1: Input parameters which vary for finite element model.

Engine-to-Engine Cycle Parameters				
Parameter	Nominal Value	Units	%(μ) 3σ Deviation	Lilliefors P-value
$T_{41,engine}$	1	normalized	1.47	0.137
$\Delta RTDF_{,engine}$	$(T_0(r)-T_{41})/T_{41}$	normalized	10	N/A
$W_{41,engine}$	1	normalized	0.61	0.099
$T_{3,engine}$	0.42	normalized	0.88	>0.2

Blade-to-Blade Flow Network Parameters				
Parameter	Nominal Value	Units	%(μ) 3σ Deviation	Lilliefors P-value
$m_{cool,blade*}$	1	normalized	7.31	0.040
$D_{SS,LE,blade}$	1	normalized	4.62	N/A
$D_{PS,LE,blade}$	1	normalized	4.62	N/A
$D_{PS,CN,blade}$	1	normalized	4.62	N/A
$D_{PS,TE,blade}$	1	normalized	4.62	N/A
*mass flow variability desired provided by variability in D_{films}				

Blade-to-Blade Conduction Parameters				
Parameter	Nominal Value	Units	%(μ) 3σ Deviation	Lilliefors P-value
$k_{sub,blade}$	1	normalized	10	N/A
$coreshift_{,blade*}$	0.0	N/A; 3σ=30% t_{wall}		N/A
$k_{tbc,blade}$	1	normalized	10	N/A
$t_{tbc,blade}$	1	normalized	20	N/A
* a positive value of core shift,blade corresponds to a thin PS				

Statistical data sets were obtained for as many parameters as possible, including cycle parameters (69 engine data set) and bench check mass flow (487 blade data set). The MATLAB Distribution Fitting Tool was used to find the best-fit analytical distribution. All the parameters were found to be best-fit by a normal distribution, with the P-value from the Lilliefors-modified Kolmogorov-Smirnov test [11] presented in Table 1. Correlation coefficients for the cycle parameters were determined and are presented in Table 2. For parameters not amenable to obtaining measured data, typical baseline values were used for the mean values and best estimates were made for the standard deviation of the assumed normal distributions.

The radial temperature distribution function $\Delta RTDF_{engine}$ requires some explanation. Figure 4 shows typical values of normalized T_0 at five locations along the span, the average which determines T_{41}. There is thus variability in the baseline inlet temperature with span: the lowest temperature is at the root, and the maximum is near mid-span. $\Delta RTDF_{engine}$ acts as a scaling parameter upon the difference between T_0 and T_{41} at each span, while keeping the same mean value for T_{41}.

Table 2: Correlation coefficients of input parameters.

$\rho_{i,j}$	$T_{3,eng}$	$T_{41,eng}$	$W_{41,eng}$
$T_{3,eng}$	+1	-0.62	+0.54
$T_{41,eng}$	-0.62	+1	-0.55
$W_{41,eng}$	+0.54	-0.55	+1

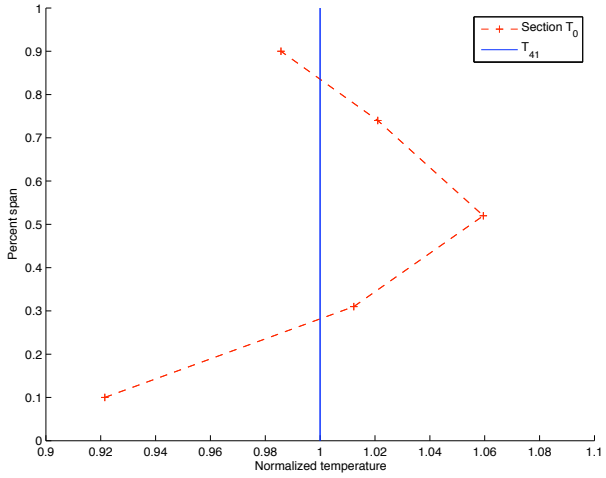

Figure 4: Typical radial temperature distribution function.

Also, it should be noted that variability in $\dot{m}_{cool,bench,blade}$ was available, but not the variability in input parameters to the flow solution which cause this variability. It is assumed that all the holes in each row of film cooling have the same diameter and the variability in hole diameter for the different rows are independent, but have the same value of σ_D. With this assumption, the variability in film hole diameter is essentially due to misalignment of the blade and the hole-cutting device. A Monte Carlo technique utilizing the multi-pass flow network model was used to determine σ_D, such that the variability of the normalized $\sigma(\dot{m}_{cool,bench,blade})$=0.0244, as observed in the sample data.

FLOW NETWORK MODEL

To supply boundary conditions to the finite element thermal model, a flow submodel of the coolant multi-pass network is first

pursued. The flow network model is shown in Figure 2. ANSYS incompressible FLUID116 elements [12] along with an average density and multiple different types of loss coefficients k allow for a quasi-compressible model to be constructed in the rotating frame of reference. Loss coefficients k dictate the velocity in each element by:

$$v = \frac{1}{\sqrt{k}} \frac{2\Delta p}{\rho}. \quad (1)$$

Three different types of losses are included: $k_{1,friction}$ is associated with frictional losses in a straight continuous duct, $k_{2,additional}$ are losses to model entrance-effects and duct-bend losses, and $k_{3,exit}$ is associated with discharge losses.

CAD/CAPRI MODEL

In order to facilitate automated regeneration of the geometry, a parametric CAD model is necessary as shown in Figure 1. The modeling is designed to capture the nature of the manufacturing process, in that the core is subtracted from the airfoil (corresponding to the removal of a wax core). The individual film cooling holes are replaced with slots so that constant-z sections always lead to a slot with width equal to the diameter of the hole. This model created in UniGraphics NX3 allows for modification of most parameters. As a proof-of-concept, only $coreshift_{blade}$ of the model varies, constraining the model such that the number and ordering of faces remains the same for any regeneration. From Table 1, coreshift$_{blade}$ shifts the core toward the pressure surface for positive values and toward the suction surface for negative values. In order to ensure robust regeneration, random numbers generated greater than +4σ are mapped to +4σ and random numbers less than -4σ are mapped to -4σ.

FINITE ELEMENT THERMAL MODEL

Using the constant-z sections provided by CAPRI, a finite element thermal model can be created as shown in Figure 3. Second-order ANSYS PLANE35 elements are used to mesh the sections, which are connected via SURF151 elements with an extra convection node to FLUID116 elements for heat exchange between the cooling flow and the blade. The mass flows calculated from the model of Figure 2 are aggregated and mapped to the nearest element corresponding to the section model. Exterior heat transfer loads are also modeled using SURF151 elements.

The external flow solution was calculated by the OEM for the baseline model with external heat transfer coefficients of the form $\mathrm{Re}^{0.8}$ scaled for the probabilistic model by:

$$h_h(W_{41}) \propto Re^{0.8} = \left(\frac{W_{41,engine}}{W_{41,engine,baseline}} \right)^{0.8}. \quad (2)$$

The presence of a thermal barrier coating (TBC) is accounted for by scaling the external heat transfer coefficients provided by the baseline model. The following relation assumes that the heat flux vectors are everywhere normal to the blade surface:

$$h_{tbc} = \frac{h}{1+Bi}, \quad (3)$$

where

$$Bi = \frac{ht_{tbc}}{k_{tbc}}. \quad (4)$$

The input parameters of Table 1 enter the model in the following ways:

- $T_{41,engine}$, and $T_{3,engine}$ scale the relevant convection temperatures in the thermal finite element model
- $W_{41,engine}$ scales the external heat transfer coefficient
- $\Delta RTDF_{engine}$ along with $T_{41,engine}$ determines the turbine inlet temperature at each span-wise location
- $k_{sub,blade}$ is directly entered as a material constant in the finite element thermal model
- $k_{tbc,blade}$ and $t_{tbc,blade}$ are used to recalculate the scaled external heat transfer coefficient accounting for the presence of TBC as indicated in Equations 3 and 4
- CAPRI handles the variable position of the core for each blade automatically.

Presented in Figures 5a-5c are the solutions for the normalized temperatures of the midspan (section 3) corresponding to the unshifted baseline and a shift of the core to +3σ and -3σ.

CREEP NON-CONFORMANCE

Blade non-conformance to a minimum acceptable creep life is predicted to occur if $T_{average,section}$ of section 2 exceeds a critical value. This critical value is hypothetically chosen to be the B_{90} temperature, implying that 10 percent of the engines will contain at least one blade with a temperature higher than the critical non-conformance temperature. An engine is assumed to nonconform if it has at least one non-conforming blade. The thermal model was chosen to predict blade life based on creep because a stress model to investigate other non-conformance mechanisms would be too computationally expensive for probabilistic analysis and proprietary lifing algorithms were not available.

PROPOSED TOLERANCING SCHEMES

The current state of manufacturing of a first-stage turbine blade is such that most tolerances involved are minimized under

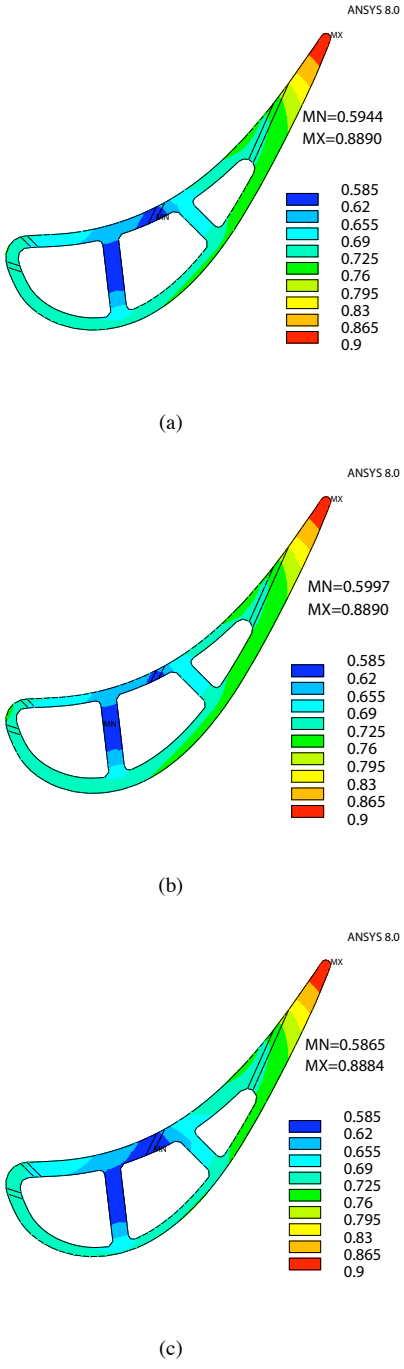

Figure 5: Section 3 normalized temperature distribution for (a) baseline unshifted model, (b) coreshift=+3σ, and (c) coreshift=-3σ.

the constraint that the parts be economically feasible to produce. Non-conformances in the field could likely be avoided by substantially reducing the acceptable manufacturing tolerances, but would likely necessitate a more expensive manufacturing technique to yield a satisfactory number of parts. However, by utilizing more stringent tolerances and thus rejecting a small number of additional parts, costly in-service non-conformances can be avoided with minimal impact to part yield. This paper will deal with not including units from the tail of each input parameter's distribution, the so called "bad-range", which causes the engine to be more likely to exhibit a non-conformance. In practice, the implementation of this scheme involves not building blades from the bad-range of a blade-to-blade level parameter and/or not shipping an engine exhibiting a parameter from the bad-range of an engine-to-engine level parameter at pass-off test. Engines found to have a bad-range engine-to-engine level parameter could be reworked to address the bad-range parameter before being returned to the pass-off test.

SENSITIVITY ANALYSIS AND RESPONSE SURFACE

A linear sensitivity analysis is the simplest response surface that can be constructed. A fractional-factorial quadratic response surface adds quadratic interaction effects. The response surface for the creep indicator, section 2 $T_{average,section}$, is presented in Table 3. For interpretation of the sensitivity analysis, the linear terms have been sorted in descending order of response magnitude. In order to reduce runs for the fractional-factorial response surface, $W_{41,eng}$ was omitted based on a 0.242 K one-factor-at-a-time response, the smallest of the engine-to-engine responses.

MONTE CARLO FLEET ANALYSIS

While the response surfaces created in the previous section are appropriate for determining effects and interactions, further analysis is required to determine how the blade-to-blade and engine-to-engine level parameters combine probabilistically to affect the operation of a fleet of engines. The most conservative approach is to use the finite element model to explicitly model a random, though correlated as appropriate per Table 2, set of 70 blades per engine in all of the 500 engines in the fleet. The computational expense of these 35,000 models is approximately one month of run time for a single CPU. It is also noted that response surfaces are amenable to efficient simulations of an entire fleet of engines. Solution time is trivial for the algebraic calculations required, such that even large fleets of engines can be constructed. The explicit finite element model, fractional-factorial response surface and one-factor-at-a-time response surface will all be presented. For consistency and comparison, the same random numbers are used for all models. A flow chart of the process is included in Figure 6 to show all of the steps required.

Table 3: Linear sensitivity analysis and fractional factorial response surface of creep indicator, section 2 $T_{average,section}$.

Linear Terms:

	β_i (K)
$D_{PS,TE,bld}$	-5.937
$T_{41,eng}$	+3.670
$t_{tbc,bld}$	-2.820
$coreshift_{bld}$	+1.891
$k_{tbc,bld}$	+1.409
$T_{3,eng}$	+1.054
$D_{PS,LE,bld}$	-0.610
$D_{SS,LE,bld}$	-0.564
$\Delta RTDF_{eng}$	+0.400
$W_{41,eng}$	+0.242
$D_{PS,CN,bld}$	-0.313
$k_{sub,bld}$	+0.139

Second Order Terms:

$\beta_{i,j}$ (K)	$T_{41,eng}$	$\Delta RTDF_{eng}$	$T_{3,eng}$	$D_{SS,LE,bld}$	$D_{PS,LE,bld}$	$D_{PS,CN,bld}$	$D_{PS,TE,bld}$	$k_{sub,bld}$	$coreshift_{bld}$	$k_{tbc,bld}$	$t_{tbc,bld}$
$T_{41,eng}$	-3.41e-04	-1.17e-05	-1.64e-04	-4.68e-03	-5.05e-03	-2.59e-03	-4.80e-02	+1.13e-03	+1.60e-02	+1.14e-02	-2.29e-02
$\Delta RTDF_{eng}$	-	-3.41e-04	-1.17e-05	-3.63e-04	-4.26e-04	-3.24e-04	-6.24e-03	-1.17e-05	+3.09e-03	+1.48e-03	-2.94e-03
$T_{3,eng}$	-	-	+1.59e-04	+1.22e-03	+1.30e-03	+7.42e-04	+1.16e-02	-2.89e-04	-4.25e-03	-2.78e-03	+5.58e-03
$D_{SS,LE,bld}$	-	-	-	+1.16e-03	+1.49e-02	+1.42e-02	+2.16e-02	-2.05e-03	+1.07e-02	-4.49e-04	+8.40e-04
$D_{PS,LE,bld}$	-	-	-	-	+2.16e-03	+1.47e-02	+2.26e-02	-2.58e-03	+3.30e-02	-5.51e-04	+1.06e-03
$D_{PS,CN,bld}$	-	-	-	-	-	+1.17e-02	+4.75e-02	-6.95e-04	+1.44e-03	-3.91e-06	+3.91e-06
$D_{PS,TE,bld}$	-	-	-	-	-	-	+2.24e-01	-8.27e-03	-2.55e-02	+2.49e-03	-4.99e-03
$k_{sub,bld}$	-	-	-	-	-	-	-	-3.34e-03	-3.58e-03	+2.95e-03	-5.94e-03
$coreshift_{bld}$	-	-	-	-	-	-	-	-	-2.43e-02	+5.47e-04	-1.05e-03
$k_{tbc,bld}$	-	-	-	-	-	-	-	-	-	-4.23e-02	+7.48e-02
$t_{tbc,bld}$	-	-	-	-	-	-	-	-	-	-	+1.92e-02

COMPARISON OF FINITE ELEMENT MODELS TO RESPONSE SURFACE MODELS

Since the same random numbers were used, the errors of both the one-factor-at-a-time and the fractional-factorial response surfaces relative to the finite element solutions, ($T_{average,section,RS}$-$T_{average,section,FE}$), could be computed for the 35,000 blade Monte Carlo simulation. Histograms of the error of both response surfaces are plotted in Figure 7. The mean and standard deviation of the one-factor-at-a-time analysis are $\mu(error)$=-0.172 K and $\sigma(error)$=0.360 K. The second-order terms of the fractional-factorial response surface significantly improve upon the approximation to the finite element results, such that the mean and standard deviation of the error are $\mu(error)$=-0.001 K and $\sigma(error)$=0.039 K. The excellent a posteriori agreement between the Monte Carlo simulations on the fractional-factorial response surface and the finite element runs indicate that, for this heat transfer problem, the fractional-factorial response surface likely yields sufficient resolution.

QUANTIFYING PARAMETER EFFECTS

A common, deterministic approach is to rank the sensitivity of an output parameter (e.g. $T_{average,section}$) to a change in each input. This is easily done by ranking the magnitude of the coefficients of a response surface. For example, according to Table 3, the most sensitive parameter would be $D_{PS,TE,bld}$, followed by $T_{41,eng}$ and $t_{tbc,bld}$. This view, however, ignores the fact that an engine consists of multiple blades (e.g. 70 first-stage turbine blades in the hypothetical engine considered) and therefore a large deviation in a blade parameter is much more likely to be present in an engine than a large deviation in an engine parameter [6,10]. More succinctly, for each engine, a blade-to-blade level parameter has 70 chances to have a larger variation while an engine-to-engine level parameter has only one chance. Table 4 shows quantitatively the difference in probability for engine-to-engine and blade-to-blade level parameters (assuming 70 blades per engine) occurring at least once per engine in a one-sided 1, 2, and 3σ normal-distribution tail. For example, a $\geq$+3σ varia-

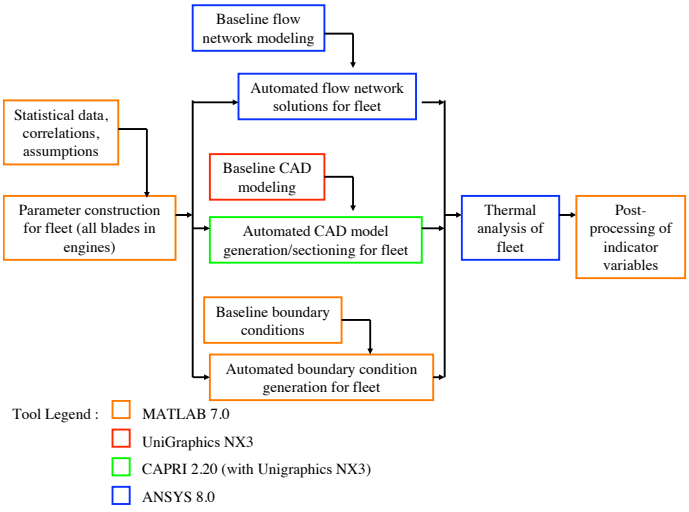

Figure 6: Flow chart showing process for fleet analysis.

tion in an engine parameter has a probability of only 0.001, while a $\geq$+3σ variation in at least one blade in an engine has a probability of 0.090, nearly 100 times larger. Thus, quantifying the importance of each parameter's variability must appropriately account for the likelihood of the parameter occurring.

Table 4: Probability of input parameter occurring in bad-range at least once in an engine containing 70 first-stage turbine blades.

Bad-Range Tail Cutoff	$Prob_{eng-to-eng}$	$Prob_{bld-to-bld}$
$>1\sigma$	0.159	1.000
$>2\sigma$	0.023	0.800
$>3\sigma$	0.001	0.090

The quantification method proposed here is based on classifying engine non-conformances. Engine non-conformance is assumed to occur when the non-conformance indicator (section 2 $T_{average,section}$) is outside an acceptable range for at least one blade. For example, if one blade of an engine has an average section temperature which is larger than some pre-determined threshold, the engine is non-conforming. The classification of engine non-conformances begins by assigning each input parameter a bad-range as described previously. Checking for a non-conformance as a result of an engine-to-engine level parameter being in the bad-range is trivial. However, for blade-to-blade level parameters, each of which occurs 70 times in an engine,

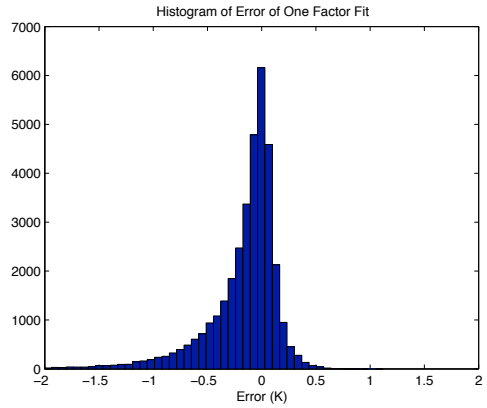

(a)

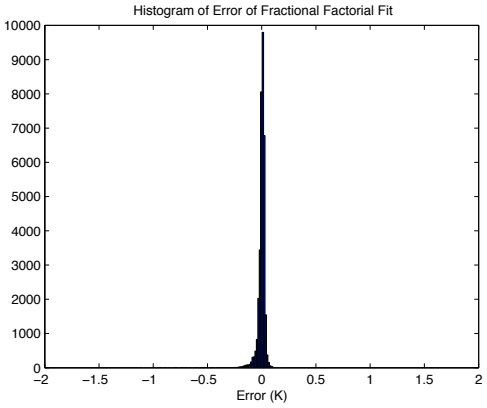

(b)

Figure 7: Histogram of error of (a) one-factor-at-a-time; (b) fractional-factorial response surfaces relative to finite element creep indicator solutions.

a more complex classification scheme is required. The broadest class is labelled "correlation" and a non-conforming engine is in this class for a specific blade-to-blade level input parameter if it has at least one blade with this input parameter in a bad-range. This correlation class is then broken into three more restrictive classes:

- Conclusive: All non-conforming blades in engine have blade-level parameter in bad-range.
- Contributing: Engine has more than one non-conforming blade, but not all non-conforming blades have blade-level parameter in bad-range.
- Coincidence: Engine is non-conforming but none of the non-conforming blades have blade-level parameter in bad-range.

In the remainder of this paper, conclusive non-conformances are used to rank the relative importance of blade-to-blade and engine-to-engine level parameters. Note that engine-to-engine level parameters are always conclusive when the engine is non-conforming and the engine-level parameter is in its bad-range.

CONCLUSIVE ENGINE NON-CONFORMANCE RESULTS

To compare the engine-to-engine and blade-to-blade level parameters directly, the number of conclusive engine non-conformances occurring for the subset of engines which have an input parameter in the bad-range are presented in Table 5. Since the critical non-conformance temperature was hypothetically defined to be at the B_{90} level, 50 engines from the 500 engine baseline fleet are non-conforming, which is the theoretical maximum of any entry in Table 5.

At this point, it is appropriate to compare the values in Table 5 between engine-to-engine and blade-to-blade level parameters. These values represent the maximum theoretical number of engines which could be salvaged by a tolerancing scheme which would replace the input parameters in the bad-range. In Table 5, and in subsequent tables, tolerancing ranges which have a potential to salvage more than 20 of the finite element-modeled engines (40% of the non-conforming engines in the fleet) are highlighted in yellow. The discussion initially refers to the explicit finite element simulations.

The parameter with the largest number of conclusive engine non-conformances given the parameter is in the bad-range is $D_{PS,TE,bld}$ which exhibited 48 conclusive engine non-conformances at the 1σ level and 44 conclusive engine non-conformances at the 2σ level. Note that the strongest engine-to-engine level parameter was $T_{41,eng}$ with 22 conclusive engine non-conformances at the 1σ level and 3 conclusive engine non-conformances at the 2σ level. At the 1σ level, $T_{41,eng}$ only exhibits 0.46 of the conclusive engine non-conformances that $D_{PS,TE,bld}$ does. At the 2σ level, this ratio is only 0.07. Both of these values are smaller than the 0.618 ratio of the linear sensitivities between the two parameters presented in Table 3. Also, note that the input parameter $t_{tbc,bld}$ exhibits 27 conclusive engine non-conformances at the 1σ level, which is more than the 22 conclusive engine non-conformances from $T_{41,eng}$. That is to say, the order of the Pareto-ranking of these parameters is different than the linear sensitivity ranking suggests as presented in Table 3. The expected effect of an increased importance of blade-to-blade level parameters (relative to what might be incorrectly concluded from a linear sensitivity analysis) is confirmed.

Another important trend is the relative strength of $\dot{m}_{cool,bld}$ compared to $D_{PS,TE,bld}$. At the 1σ level, the ratio of conclusive engine non-conformances is 0.92 when comparing the 44 conclusive engine non-conformances of $\dot{m}_{cool,bld}$ to the 48 conclusive engine non-conformances of $D_{PS,TE,bld}$. However, by the 2σ level, this ratio has reduced to 0.59 (26:44). This implies that even though the aggregate cooling flow through the blade, $\dot{m}_{cool,bld}$, is a strong parameter, the diameter of the film cooling hole at the trailing edge, $D_{PS,TE,bld}$, is an even stronger parameter. This is because not only does $D_{PS,TE,bld}$ tend to act as the meter of the blade, but it also affects the heat transfer in a critical location, the trailing edge tip.

Table 5 also contains the results for the fractional-factorial response surfaces, the one-factor-at-a-time response surface. What is important is that with the exception of some slight discrepancies related to the parameter $D_{PS,TE,bld}$, the fractional-factorial response surface matches the predictions of the finite element solution. Excellent agreement is to be expected because of the small error of the fractional-factorial response surface shown in Figure 7b. However, since $\dot{m}_{cool,bld}$, is an intermediate output variable of the finite element flow-network model, the fractional-factorial response surface does not yield important information regarding the comparison of $\dot{m}_{cool,bld}$ to $D_{PS,TE,bld}$. Also note the excellent trend-wise agreement between the finite element simulations and the one-factor-at-a-time response surface.

CONFIDENCE RANGE ANALYSIS

One important question which needs to be answered is whether the conclusions drawn from the 500 engine sample are statistically significant. Probability theory offers a means to answer this question. Specifically, an estimate $\hat{P}$ of the probability P of conclusive engine non-conformances from an input parameter in the bad-range is given by:

$$\hat{P}\left(\text{non-conformance}_{\text{engine,conclusive}}\text{for an input}\right) = \quad (5)$$

$$\frac{\text{number of conclusive engine NC for an input}}{\text{number of engines}}.$$

For a (1-α) confidence interval, the range of the probability P can be expressed as a function of the sample probability [13]:

$$\hat{P}-Z_{\frac{\alpha}{2}}\sqrt{\frac{\left(\hat{P}\right)\left(1-\hat{P}\right)}{\text{number of engines}}}<P<\hat{P}+Z_{\frac{\alpha}{2}}\sqrt{\frac{\left(\hat{P}\right)\left(1-\hat{P}\right)}{\text{number of engines}}}, \quad (6)$$

where $Z_{\frac{\alpha}{2}}$ is the area under the $\frac{\alpha}{2}$ tail of the normal curve.

The range of the probability estimated by the sample probability is presented in Table 6 to 0.90 confidence. The ranges presented indicate some overlap among the ranges of interest which are highlighted.

Table 5: Number of conclusive engine non-conformances for creep indicator.

Finite Element Simulations

Cycle Parameters: Range	# (Conclusive) Engine NC Given BR			
	$T_{41,eng}$	$\Delta RTDF_{eng}$	$W_{41,eng}$	$T_{3,eng}$
>1σ	22	10	8	12
>2σ	3	0	0	2
>3σ	0	0	0	1

Flow Network Parameters: Range	# Conclusive Engine NC Given BR				
	$D_{SS,LE,bld}$	$D_{PS,LE,bld}$	$D_{PS,CN,bld}$	$D_{PS,TE,bld}$	$m_{cool,bld}$
>1σ	15	7	9	48	44
>2σ	4	1	1	44	26
>3σ	1	1	0	16	10

Conduction Parameters: Range	# Conclusive Engine NC Given BR			
	$k_{sub,bld}$	cr-shft$_{bld}$	$k_{tbc,bld}$	$t_{tbc,bld}$
>1σ	7	14	18	27
>2σ	0	4	3	7
>3σ	0	1	0	2

Fractional-Factorial Response Surface

Cycle Parameters: Range	# (Conclusive) Engine NC Given BR			
	$T_{41,eng}$	$\Delta RTDF_{eng}$	$W_{41,eng}$	$T_{3,eng}$
>1σ	22	10	8	12
>2σ	3	0	0	2
>3σ	0	0	0	1

Flow Network Parameters: Range	# Conclusive Engine NC Given BR				
	$D_{SS,LE,bld}$	$D_{PS,LE,bld}$	$D_{PS,CN,bld}$	$D_{PS,TE,bld}$	$m_{cool,bld}$
>1σ	15	7	9	49	N/A
>2σ	4	1	1	45	N/A
>3σ	1	1	0	16	N/A

Conduction Parameters: Range	# Conclusive Engine NC Given BR			
	$k_{sub,bld}$	cr-shft$_{bld}$	$k_{tbc,bld}$	$t_{tbc,bld}$
>1σ	7	14	18	27
>2σ	0	4	3	7
>3σ	0	1	0	2

One-Factor-at-a-Time Response Surface

Cycle Parameters: Range	# (Conclusive) Engine NC Given BR			
	$T_{41,eng}$	$\Delta RTDF_{eng}$	$W_{41,eng}$	$T_{3,eng}$
>1σ	24	8	10	13
>2σ	4	0	0	3
>3σ	0	0	0	1

Flow Network Parameters: Range	# Conclusive Engine NC Given BR				
	$D_{SS,LE,bld}$	$D_{PS,LE,bld}$	$D_{PS,CN,bld}$	$D_{PS,TE,bld}$	$m_{cool,bld}$
>1σ	14	6	7	48	N/A
>2σ	4	2	0	40	N/A
>3σ	1	1	0	10	N/A

Conduction Parameters: Range	# Conclusive Engine NC Given BR			
	$k_{sub,bld}$	cr-shft$_{bld}$	$k_{tbc,bld}$	$t_{tbc,bld}$
>1σ	6	14	22	28
>2σ	0	5	4	8
>3σ	0	2	1	3

The 500 engine fleet size is determined to be marginally sufficient for parameter-ranking purposes as a result of the following conclusions:

- $D_{PS,TE,bld}$ at 1σ and 2σ is statistically better than $T_{41,eng}$ at 1σ.
- $t_{tbc,bld}$ at 1σ is not statistically better than $T_{41,eng}$ at 1σ.
- $D_{PS,TE,bld}$ is better than $t_{tbc,bld}$ when comparing the same σ-level.

Table 6: Probability (0.90 confidence) of conclusive engine non-conformance from an input for creep indicator of finite element simulations.

Cycle Parameters

Range	P(non-conformance$_{engine,(conclusive)}$ for an input)			
	$T_{41,eng}$	$\Delta RTDF_{eng}$	$W_{41,eng}$	$T_{3,eng}$
>1σ	0.044±0.015	0.020±0.010	0.016±0.009	0.024±0.011
>2σ	0.006±0.006	0.000±0.000	0.000±0.000	0.004±0.005
>3σ	0.000±0.000	0.000±0.000	0.000±0.000	0.002±0.003

Flow Network Parameters

Range	P(non-conformance$_{engine,(conclusive)}$ for an input)				
	$D_{SS,LE,bld}$	$D_{PS,LE,bld}$	$D_{PS,CN,bld}$	$D_{PS,TE,bld}$	$m_{cool,bld}$
>1σ	0.030±0.013	0.014±0.009	0.018±0.010	0.096±0.022	0.088±0.021
>2σ	0.008±0.007	0.002±0.003	0.002±0.003	0.088±0.021	0.052±0.016
>3σ	0.002±0.003	0.002±0.003	0.000±0.000	0.032±0.013	0.020±0.010

Conduction Parameters

Range	P(non-conformance$_{engine,(conclusive)}$ for an input)			
	$k_{sub,bld}$	cr-shft$_{bld}$	$k_{tbc,bld}$	$t_{tbc,bld}$
>1σ	0.014±0.009	0.028±0.012	0.036±0.014	0.054±0.017
>2σ	0.000±0.000	0.008±0.007	0.006±0.006	0.014±0.009
>3σ	0.000±0.000	0.002±0.003	0.000±0.000	0.004±0.005

TOLERANCE ASSESSMENT

The analysis of variability in Table 5 is limited to providing the maximum theoretical number of engines which could be salvaged by implementing a tolerancing scheme. In addition to addressing input parameters which would cause non-conformances in the field, any tolerancing scheme will likely replace some units which would not have exhibited a non-conformance in the field. One noteworthy example is that in a one-factor blade-to-blade tolerancing scheme there is a possibility for bad-range blades which would not have non-conformed in a specific engine to be replaced by blades which do non-conform in that engine, likely as a result of a different parameter being in its bad-range. By augmenting the Monte Carlo simulations with additional simulations to allow for toleranced units, an efficient cost-benefit analysis of tolerancing alternatives can be performed.

SALVAGED ENGINE NON-CONFORMANCES

The B_{90} non-conformance criteria presented earlier implies that the baseline design is expected to have 10% of the engines in the fleet non-conform, or 50 non-conforming engines for the 500 engine fleet. For a tolerancing scheme, the number of salvaged engines is the number of engines less than the expected number of 50 engine non-conformances. By post-processing the creep indicator of the finite element augmented Monte Carlo simulations, the number of engines salvaged by various tolerancing schemes is calculated and presented in Tables 7 and 8.

Table 8 represents a single-factor tolerancing scheme, where separate fleets are constructed while tolerancing one parameter at a time. In practice, this could be implemented by rejecting the bad-range blades before they are ever built into the engines. Comparisons are included between the lower-fidelity response surfaces and the finite element model. The cooling flow parameters, $D_{PS,TE,bld}$ and $\dot{m}_{cool,bld}$ are the most effective blade-to-blade level parameters to tolerance. For example, rejecting $D_{PS,TE,bld}$

Table 8: Number of salvaged engine non-conformances for creep indicator of single-factor tolerancing.

	Cycle Parameters				Flow Network Parameters					Conduction Parameters			
	Tolerance	# of Salvaged Engines				Tolerance	# of Salvaged Engines					Tolerance	# of Salvaged Engines			
		$T_{41,eng}$	$\Delta RTDF_{eng}$	$W_{41,eng}$	$T_{3,eng}$		$D_{SS,LE,bld}$	$D_{PS,LE,bld}$	$D_{PS,CN,bld}$	$D_{PS,TE,bld}$	$m_{cool,bld}$		$k_{sub,bld}$	cr-shft$_{bld}$	$k_{tbc,bld}$	$t_{tbc,bld}$
Finite Element Simulations	>1σ	22	5	7	11	>1σ	9	4	6	48	44	>1σ	0	9	15	21
	>2σ	3	0	-1	1	>2σ	3	-1	-1	44	26	>2σ	-3	3	2	4
	>3σ	0	0	0	1	>3σ	1	1	-1	16	10	>3σ	0	1	0	1
Fractional-Factorial Response Surface	>1σ	22	5	7	11	>1σ	9	4	6	49	N/A	>1σ	0	9	15	21
	>2σ	3	0	-1	1	>2σ	3	-1	-1	45	N/A	>2σ	-3	3	2	4
	>3σ	0	0	0	1	>3σ	1	1	-1	16	N/A	>3σ	0	1	0	1
One-Factor-at-a-Time Response Surface	>1σ	23	2	7	10	>1σ	8	2	4	48	N/A	>1σ	1	9	20	23
	>2σ	4	0	-1	2	>2σ	3	1	-2	39	N/A	>2σ	-2	4	3	6
	>3σ	0	0	0	1	>3σ	1	1	0	10	N/A	>3σ	0	2	1	3

Table 7: Number of salvaged engine non-conformances for creep indicator of two-factor tolerancing of finite element simulations.

	# of Salvaged Engines		
Tolerance	$D_{PS,TE,bld}$>1σ	$D_{PS,TE,bld}$>2σ	$D_{PS,TE,bld}$>3σ
$T_{41,eng}$>1σ	50	49	33
$T_{41,eng}$>2σ	49	47	19
$T_{41,eng}$>3σ	48	44	16

at the 2σ level salvaged 44 engines, while a marginal improvement of 48 salvaged engines is realized at the 1σ level. Another blade-to-blade parameter of interest is $\dot{m}_{cool,bld}$, which salvaged 26 engines at the 2σ level, while realizing a substantial improvement to 44 engines at the 1σ level. Also, it should be noted that while overall cooling flow variability, $\dot{m}_{cool,bld}$, is important, further data of flow variability through the metering passage at the trailing edge can lead to even more effective tolerancing.

Tolerancing schemes need not be limited to single-factor tolerancing. In practice, a two-factor scheme could be implemented by first rejecting bad-range blades from being built into an engine and then reworking the engines which exhibit a bad-range engine-to-engine level parameter which would become apparent during a pass-off test before the engine is shipped to a customer. Numerically, the augmented engine framework does not allow for the blades from an engine with a bad-range engine-to-engine level parameter to be reused, whereas in practice the blades could be reused. However, there is no statistical risk to this discrepancy, since the blades are not modeled to affect the engine-to-engine level parameters, and there is no statistical preference of the blades between engines.

Table 7 investigates a fleet constructed in such a way that not only rejects the bad-range of the strongest blade-to-blade level parameter, $D_{PS,TE,bld}$, but also doesn't ship engines in which strongest engine-to-engine level parameter, $T_{41,eng}$, is in the bad-range. It is evident, that there is a compounding effect due to the interaction of ensuring that no engine contains either of these parameters in their respective bad-ranges. Simultaneously tolerancing $D_{PS,TE,bld}$ and $T_{41,eng}$ both at the 2σ level salvages 47 of the 50 expected non-conforming engines and is highlighted as a recommended tolerancing scheme for profitability reasons to be presented later.

COST STRUCTURE

For the purpose of evaluating cost ramifications related to blade robustness a simple cost structure model was employed:

- The cost of a non-conformance in the field is assumed to have a cost of A.
- The cost of manufacturing each blade is B.
- The cost of rejecting an engine for rework as a result of a failed pass-off test at the manufacturer is C.

A tolerancing scheme can be characterized by $\alpha_{salvage}$, the number of non-conformances salvaged from a fleet which would have $\alpha_{baseline}$ non-conformances if nothing is done, β blades that are manufactured but never used due to a blade-to-blade level parameter being in the bad-range, and γ engines that need to be reworked due to an engine-to-engine parameter being in the bad-range. For a fleet subject to a tolerancing scheme, the relevant costs are

- the avoided cost of non-conformances in the field is $\alpha_{salvage}$A,
- the cost of the "bad-range" blades manufactured but not used is βB,
- the cost of engines requiring rework is γC.

While the true value of each of these costs is proprietary, characteristic ratios of the costs can be used. These non-

dimensional cost ratios (B/A, C/A) are varied in [7] to demonstrate that even under wildly different cost assumptions, the recommended tolerancing schemes are still money-making initiatives. By normalizing the costs involved by the cost of the field non-conformances which would occur if nothing is done, $\alpha_{baseline}$A, a net normalized profit π can be calculated from

$$\pi = \frac{\alpha_{salvage}}{\alpha_{baseline}} - \frac{(\beta B + \gamma C)}{\alpha_{baseline} A}. \quad (7)$$

If π is greater than zero, the tolerancing-scheme is a money-making initiative. A maximum theoretical value of π=1 implies that all engines which would have been non-conforming were salvaged by a tolerancing scheme which cost nothing to implement. It should be noted, that a money-losing initiative is not limited to π=-1. To calculate the net-profit in units of currency, π is simply multiplied by $\alpha_{baseline}$A.

PROFITABILITY ANALYSIS

To determine if a tolerancing scheme is a money-making initiative under an assumption that the ratios of the costs are
$\frac{cost\ of\ blade}{cost\ of\ engine\ non-conformance\ in\ field} = \frac{B}{A} = 0.001$,
$\frac{cost\ to\ rework\ engine}{cost\ of\ engine\ non-conformance\ in\ field} = \frac{C}{A} = 0.1$,
the normalized profitabilities of the tolerancing schemes can be calculated using the simple cost model described in Equation 7. These normalized profitabilities are presented in Table 9. It is noted that two-factor tolerancing can provide the largest normalized profability with the non-dimensional costs assumed.

CONCLUSIONS

This work demonstrated that modern computing resources and software allows for automated analysis which can enable probabilistic simulations on a large scale. Specifically applied to a first-stage turbine blade, it was demonstrated that:

- A parameterized finite element thermal model can be constructed allowing for robust simulation of multiple instances.
- Response surface models can be used to approximate the trend-wise behavior of a finite element thermal model for a fleet of engines.
- Monte Carlo techniques can allow for an analysis of input parameters that occur at multiple levels to be analyzed simultaneously, and tolerancing schemes of the input parameters ranked accordingly. This exposes a key weakness of linear-sensitivity analyses when input parameters occur at different levels.
- Monte Carlo techniques indicate that a two-factor simultaneous tolerancing scheme of $D_{PS,TE,bld}$ and $T_{41,eng}$ is the most promising for reducing creep-induced non-conformances.

Table 9: Normalized profitability for one and two factor tolerancing for creep indicator of finite element simulations.

Cycle Parameters

Tolerance	Normalized Profitability, π			
	$T_{41,eng}$	$\Delta RTDF_{eng}$	$W_{41,eng}$	$T_{3,eng}$
>1σ	0.276	-0.106	-0.044	0.042
>2σ	0.048	-0.020	-0.044	-0.008
>3σ	0.000	0.000	-0.002	0.018

Flow Network Parameters

Tolerance	Normalized Profitability, π				
	$D_{SS,LE,bld}$	$D_{PS,LE,bld}$	$D_{PS,CN,bld}$	$D_{PS,TE,bld}$	$m_{cool,bld}$
>1σ	0.047	-0.052	-0.015	0.829	0.749
>2σ	0.044	-0.035	-0.037	0.864	0.504
>3σ	0.019	0.019	-0.021	0.319	0.199

Conduction Parameters

Tolerance	Normalized Profitability, π			
	$k_{sub,bld}$	cr-shft$_{,bld}$	$k_{tbc,bld}$	$t_{tbc,bld}$
>1σ	-0.131	0.044	0.165	0.288
>2σ	-0.076	0.044	0.023	0.064
>3σ	-0.001	0.019	-0.001	0.019

Two-Factor Tolerancing

Normalized Profitability, π			
Tolerance	$D_{PS,TE,bld}$>1σ	$D_{PS,TE,bld}$>2σ	$D_{PS,TE,bld}$>3σ
$T_{41,eng}$>1σ	0.706	0.800	0.495
$T_{41,eng}$>2σ	0.837	0.912	0.367
$T_{41,eng}$>3σ	0.829	0.864	0.319

ACKNOWLEDGMENT

The first author listed would like to thank Rolls-Royce for supporting the MIT Gas Turbine Laboratory Whittle Fellowship, under which this work was completed. Also thanks to Bob Haimes and Ali Merchant for support related to CAPRI, David Walfisch for creation of the parametric CAD model and Alexander Karl for probabilistic guidance.

REFERENCES

[1] Voigt, M., Mücke, R., Vogeler, K., and Oevermann, M. "Probabilistic lifetime analysis for turbine blades based on a combined direct monte carlo and response surface approach". GT2004-53439, 2004 ASME Turbo Expo.

[2] McClung, R. C., Bernstein, H. L., Buckingham, J. P., Allen, J. M., and Touchton, G. L. "Probabilistic analyses of industrial gas turbine durability". 93-GT-427.

[3] Mücke, R. "A probabilistic desing approach to lifetime prediction for turbine blades". European Congress on Computational Methods in Applied Sciences and Engineering, ECCOMAS 2000.

[4] Volovoi, V. V., Waters, M., and Mavris, D. N. "Comparative

assessment of direct and indirect probabilistic methods for thermomechanical analysis of structural components in gas turbines". GT2003-38510, 2003 ASME Turbo Expo.

[5] Reh, S., Palfi, T., and Nemeth, N. N. "Probabilistic analysis techniques applied to lifetime reliability estimation of ceramics.". JANNAF 39th Combustion Subcommittee, 27th Airbreathing Propulsion, 21st Propulsion Systems Hazards Committee, and 3rd Modeling and Simulation Subcommittee Joint Meeting, December 2003. Available from Chemical Propulsion Information Agency.

[6] Sidwell, V., and Darmofal, D. "The impact of blade-to-blade flow variability on turbine blade cooling performance". ASME Journal of Turbomachinery, October 2005 Vol. 127.

[7] Moeckel, C. W., 2006. "Probabilistic turbine blade thermal analysis of manufacturing variability and toleranced designs". Master's thesis, Massachusetts Institute of Technology, Department of Aeronautics and Astronautics.

[8] Haimes, R., and Merchant, A. "The synergistic use of cad for tightly coupled analysis and design". AIAA 2005-4986.

[9] Incropera, F. P., and DeWitt, D. P., 2002. *Fundamentals of Heat and Mass Transfer: Fifth Edition*. John Wiley and Sons, New York, NY.

[10] Sidwell, C. V., 2004. "On the impact of variability and assembly on turbine blade cooling flow and oxidation life". Doctor of philosophy dissertation, Massachusetts Institute of Technology, Department of Aeronautics and Astronautics, June.

[11] Lilliefors, H. W., 1967. "On the kolmogorov-smirnov test for normality with mean and variance unknown". Vol. 62 of *Journal of the American Statistical Association*, pp. 399–402.

[12] "Ansys release 8.0 documentation".

[13] Walpole, R., Myers, R. H., and Myers, S., 1998. *Probability and Statistics for Engineers and Scientists: Sixth Edition*. Prentice Hall, Upper Saddle River, NJ.